Scattering of 14.5-Mev Neutrons by Complex Nuclei*

J. H. Coon, R. W. Davis, H. E. Felthauser, and D. B. Nicodemus†
Los Alamos Scientific Laboratory, University of California, Los Alamos, New Mexico
(Received February 10, 1958; revised manuscript received May 19, 1958)

New measurements of the differential elastic scattering cross sections of C, Al, Fe, Cu, Sn, Pb, and U for 14.5-Mev neutrons are reported. For Fe, Cu, Sn, and Pb the angular range from 5° to 150° was investigated with ±1° to ±3° angular resolution. For the other elements a smaller angular range was investigated. Particular effort was devoted to the problem of discriminating against inelastically scattered neutrons and methods were developed which provided an experimental energy resolution of ~500 kev. Limited differential cross section data for inelastically scattered neutrons of energy greater than 9 Mev are also presented for Fe, Cu, Sn, and Pb.

I. INTRODUCTION

During the past few years differential elastic scattering of protons and neutrons by complex nuclei has been studied experimentally at many energies between 1 and 100 Mev. The experiments have been interpreted by means of the optical model[1] of the nucleus, and interesting values of the depth, shape, and radius of the apparent nuclear potentials have been derived. Above about 10 Mev the proton experiments[2] have yielded more information than the neutron experiments because of the relatively high accuracy and wide angular range possible in the proton measurements. At lower energies many measurements[3] have been made and provide information in the energy region where proton scattering is predominantly Coulomb and therefore not indicative of the nuclear potentials. More accurate data over wider ranges of energy and angle are still desirable for further development of the theory which is beginning to incorporate spin-orbit coupling and nuclear shape.

The present article is a report of new measurements of differential elastic scattering of 14.5-Mev neutrons. Limited cross section data for inelastic scattering are also presented. More accurate elastic scattering data for protons at the roughly equivalent energy of 17 Mev are available.[4] However, experimental investigations for both neutrons and protons are certainly of value because there are probably real differences between the nuclear potentials experienced by neutrons and by protons.[5,6] Furthermore the theory for the neutron data is considerably simplified by the absence of the Coulomb potential. The neutron data yield significant values near zero degrees where the Coulomb force dominates proton scattering.

There have been several previous experiments[7–19] on neutron scattering at 14 Mev. Among the earliest was that reported by Amaldi *et al.*[7] who obtained differential cross sections for Pb in the angular range from 20° to 80°. Although their experiment was seriously limited by the low neutron source strength available, it developed an optimized ring-scattering geometry which is very useful. Subsequent measurements, using various techniques, have been made on 20 elements (excluding H, D, and He) from Be to U, though usually the experiments have covered a rather limited angular range. The earliest extensive work was that of Cross and Jarvis[3,12] who measured Bi, Cd, Ca, and Mg over the angular range from 8° to 130°. However for angles greater than 90°, their measurements for Bi and Cd were quoted with errors up to 50% and no structure was evident in their differential cross section curves for these angles. Measurements by Elliot[3,13] on five elements covered angles from 5° to 55° where the test of the theory is not as stringent as at larger angles. More recent measurements by the Livermore group[17] have covered angles from 90° to 165° for Pb, Sn, Cd, Ag, Cu, and Fe, and from 20° to 140° for Be, C, and N. The present work, begun in 1953,[3,9] covers the angular range from 5° to

* Work performed under the auspices of the U. S. Atomic Energy Commission.
† On leave from Oregon State College, Corvallis, Oregon.
[1] Feshbach, Porter, and Weisskopf, Phys. Rev. **96**, 448 (1954); L. Van Hove, Physica **22**, 979 (1956); W. B. Riesenfeld and K. M. Watson, Phys. Rev. **102**, 1157 (1956); A. E. S. Green, Phys. Rev. **102**, 1325 (1956); Melkanoff, Nodvik, Saxon, and Woods, Phys. Rev. **106**, 793 (1957); Glassgold, Cheston, Stein, Schuldt, and Erickson, Phys. Rev. **106**, 1207 (1957); A. E. Glassgold and P. J. Kellogg, Phys. Rev. **107**, 1372 (1957).
[2] N. M. Hintz, Phys. Rev. **106**, 1201 (1957). This article presents a comprehensive list of references to experimental work on proton scattering.
[3] D. J. Hughes and R. S. Carter, Brookhaven National Laboratory Report BNL-400, 1956 (unpublished).
[4] I. E. Dayton and G. Schrank, Phys. Rev. **101**, 1358 (1956).
[5] We wish to thank A. E. S. Green for discussions of this point.
[6] H. A. Bethe, Physica **22**, 945 (1956).
[7] Amaldi, Bocciarelli, Cacciapuoti, and Trabacchi, Nuovo cimento **3**, 203 (1946).
[8] J. P. Conner, Phys. Rev. **89**, 712 (1953).
[9] J. H. Coon and R. W. Davis, Phys. Rev. **94**, 785(A) (1953).
[10] J. R. Smith, Phys. Rev. **95**, 730 (1954).
[11] W. J. Rhein, Phys. Rev. **98**, 1300 (1955).
[12] W. G. Cross and R. G. Jarvis, Phys. Rev. **99**, 621(A) (1955).
[13] J. O. Elliot, Phys. Rev. **101**, 684 (1956).
[14] H. Nauta, Nuclear Phys. **2**, 124 (1956).
[15] H. A. Mehlhorn, Bull. Am. Phys. Soc. Ser. II, **1**, 56 (1956).
[16] Dolan, Fincher, Kenny, Berko, and Whitehead, Bull. Am. Phys. Soc. Ser. II, **1**, 339 (1956).
[17] Anderson, Gardner, Nakada, and Wong, Bull. Am. Phys. Soc. Ser. II, **2**, 233 (1957); *Proceedings of the International Conference on the Neutron Interactions with the Nucleus*, held at Columbia University, 1957 (to be published), Sec. IV-C4; also private communication.
[18] L. A. Rayburn, Bull. Am. Phys. Soc. Ser. II, **2**, 233 (1957).
[19] Many of the data, some of which are not elsewhere published, appear in reference 3.

150° for Pb, Sn, Cu, and Fe, and a more limited range from 5° to about 60° for U, Al, and C.

II. EXPERIMENTAL METHOD

The scattering geometry is shown in Fig. 1, where the scattering sample is shown as a thin cylindrical shell located with its axis along the line between a $T(d,n)He^4$ neutron source and a recoil-proton neutron detector. The angle between the axis of the scattering geometry and the deuteron beam was either 0° or 90°, and these orientations will be referred to as "0°-geometry" and "90°-geometry" conditions. A solid cylindrical rod of tungsten (shadow bar), mounted on the axis of the scattering ring, shielded the detector from neutrons emitted along the axis toward the detector. A small fraction of the neutrons emitted from the source with initial average energy $\bar{E}$ were elastically scattered from the ring through angles near θ toward the detector. These scattered neutrons, of average energy $\bar{E}'<\bar{E}$, lost a small fraction of their original energy to the recoiling nuclei and were detected with efficiency $\epsilon(\bar{E}')\neq\epsilon(\bar{E})$.

At the midpoints of the sample, the scattering angle is given by $\theta=2$ arc $\tan(b/D)$. Scattering angle θ was varied by varying b and D, about eight sample radii being used to cover the angular range from 5° to 150°. The value of $2D$ ranged from 11 to 30 inches.

Observations of the number of counts in the neutron detector per source neutron were made under the following three sets of conditions: A = count with scattering ring and shadow bar in place; B = count with scattering ring removed; C = count with both ring and shadow bar removed. For the 0°-geometry measurements, the count C was observed with the detector rotated on a circular arc around the $T(d,n)$ source to an angle α such that the neutron energy was equal to the energy of the elastically scattered neutrons. The neutron energy variations around the source, due to center-of-mass motion, were of convenient magnitude to permit quantitative compensation in this manner for the small energy lost by the elastically scattered neutrons. This procedure eliminated the need for detector sensitivity corrections, but required a knowledge of the relative neutron yields *vs* angle around the source. However, for the 90°-geometry measurements, the count C was observed with the position of the detector left unchanged, i.e., on the axis of the scattering geometry. For this arrangement the average energy of the detected neutrons was equal to the average energy of those incident on, rather than scattered by, the scattering sample. An explicit correc- $\epsilon(\bar{E})$ for detector sensitivity *versus* neutron energy was then required.

The quantity $(A-B)$ is the net count due to neutrons scattered by the ring, B being the background count due to neutrons scattered by the air, target holder, and nearby objects around the room. Since the background counts were negligible compared with C, as will be discussed in Sec. VI, no background correction was made to the count C, which is taken to be the count due to neutrons emitted by the source directly toward the detector. One of the chief experimental problems was to make the "signal-to-background" ratio $(A-B)/B$ as large as possible for the sake of accuracy. An attempt was made to optimize the geometry for this purpose. The number of neutrons scattered by the sample and arriving at the detector is proportional to $N/(r_1r_2)^2$. Thus this quantity should be made as large as possible with the appropriate limitations on angle spread $\Delta\theta$, and on sample thickness traversed by the neutrons. Contributions to $\Delta\theta$ by the finite size of the neutron source and the detector must be included. To optimize the geometry under these conditions, Amaldi *et al.*[7] employed barrel-shaped samples with the scattering atoms along the locus of points of equal scattering angles. In every plane through the axis joining source and detector, this locus defines a circular arc. Because of the difficulty of fabricating the barrel-shaped samples needed to fit this arc, we used thin cylindrical samples located tangent to the circle of equal scattering angles, i.e., halfway between source and detector. Approximation of the barrel shape by a short cylinder does not increase the angular spread drastically, because a considerable fraction of the over-all spread is due to the finite size of a practical source and detector.

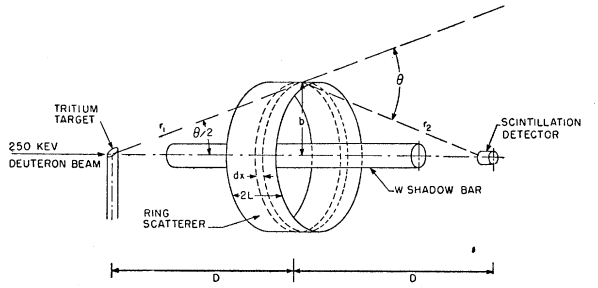

FIG. 1. Scattering geometry showing relative position of neutron source, scattering sample, neutron detector, and shadow bar.

For the purpose of minimizing the background B, the amount of extraneous scattering material in the vicinity of the experimental setup was kept to a minimum and scattering of neutrons by the air was a major contributor to the background.

Differential cross sections were evaluated from the expression

$$\sigma_e(\theta)=\frac{RL}{2ND^2}\left(\int_L^{+L}\frac{dx}{r_1^2r_2^2}\right)^{-1}\frac{n(\alpha)}{n(\theta/2)}\frac{f_1(\phi,\alpha)}{f_2(\theta/2)}\frac{e^{p/\lambda x}}{\epsilon M}, \quad (1)$$

where $R=(A-B)/C$ is the "net-over-bare" ratio, N is the number of atoms in the sample, and r_1, r_2, D, and L are dimensions given in Fig. 1. The terms following the integral term are corrections, usually not more than 5 or 10%: $n(\alpha)/n(\theta/2)$ is a correction for the laboratory yield asymmetry of the $T(d,n)$ reaction; f_1 and f_2 are

corrections for neutron flux asymmetries due to attenuation of neutrons by absorption and scattering in the target holder; ϵ is the detector-sensitivity correction referred to above; $\exp(p/\lambda_X)$ is a correction for absorption of neutrons by nonelastic collisions within the thickness t of the sample, λ_X being the mean free path for nonelastic collisions[20] and $p=t/\sin(\theta/2)$; M is a correction for multiple scattering and is not strictly separable from the factor $\exp(p/\lambda_X)$. The correction $M^{-1}\exp(p/\lambda_X)$ was calculated for some of the measurements by Monte Carlo methods.[21]

Considerable effort was devoted to the problem of discriminating against neutrons inelastically scattered with small energy loss. As will be described later, this was done by detailed study of the upper end of the pulse-height spectra A, B, and C observed from the recoil-proton detector.

The 0° and the 90° geometries referred to above have specific advantages and disadvantages when compared with one another. With the 0° geometry, the energy spread of neutrons incident on the sample is less than exists with the 90° geometry, where the energy spread increases quite rapidly with increase in scattering angle. On the other hand, with the 0°geometry, the average energy of neutrons incident on the scattering ring varies from 14.9 to 14.2 Mev as scattering angle varies from 5° to 150°, whereas with the 90° geometry the average energy is constant. However, no very rapid variation of the cross section with energy is expected in this energy range.[22] For these reasons the 90° geometry was employed only for angles up to about 70°, and the 0° geometry for angles between 20° and 150°, the large region of overlap serving as a check between the two methods.

III. NEUTRON SOURCE

Neutrons were produced by bombarding thick targets of tritium absorbed in zirconium[23] with 250-kev deuterons from a Cockcroft-Walton accelerator. Up to 300 μa of beam current were available. Total available neutron emission rate, as measured by counting the associated α particles from the $T(d,n)He^4$ reaction, was usually about 3×10^{10} neutrons per sec.

Laboratory angular asymmetry in the yield of the neutrons from the $T(d,n)$ reaction was calculated on the basis of yield isotropy in the c.m. system.[24] For the 0° geometry, the ratio $n(\alpha)/n(\theta/2)$ in Eq. (1) is the ratio of the calculated yield at the angular position α of the detector during the count C, and at the mean angular position $\theta/2$ of the circumference of the scattering ring during the count A. For the 90° geometry, the ratio $n(\alpha)/n(\theta/2)$ is equal to unity, because a simple calculation shows the average yield of neutrons incident on the scattering ring is equal to the yield at 90°, the fixed detector position. Approximate calculations of the average neutron energy $\bar{E}$ and the neutron energy spread ΔE were calculated from particle dynamics with an estimate of multiple scattering of deuterons within the thick target.[25] For the 0° geometry these quantities varied with scattering angle as shown in Fig. 2, where it is seen that ΔE was approximately ±350 kev, nearly independent of angle. For the 90° geometry $\bar{E}=14.1$ Mev was constant, independent of angle, while ΔE increased from ±150 kev at $\theta=0°$ to ±800 kev at $\theta=70°$. It is apparent that our differential cross sections should strictly be regarded as functions $\sigma_\epsilon(\theta,E)$ of neutron energy as well as angle. However, to a first approximation one may refer all the values to an arbitrarily chosen mean energy of 14.5 Mev. This point will be discussed further in Sec. XII.

There was an additional neutron flux asymmetry in the 0°-geometry measurements caused by absorption and scattering of neutrons in the target holder and immediately surrounding materials. The factors f_1 and f_2, which correct for these attenuation effects, were determined by a series of direct measurements of the relative yield of neutrons emerging through the target holder as a function of the angular position of the detector around the target holder. By a graphical

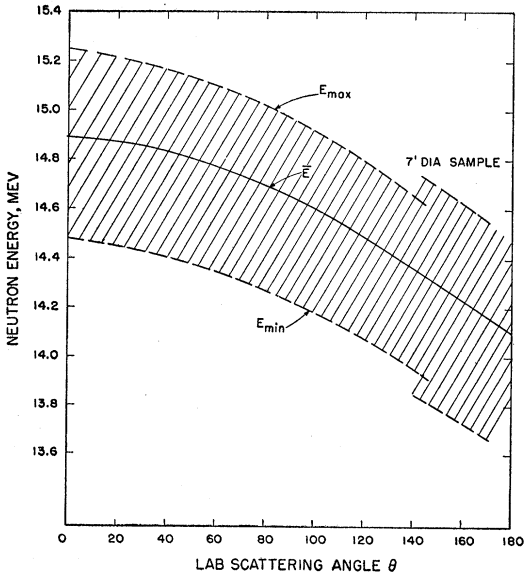

FIG. 2. Variation of average neutron energy $\bar{E}$ with lab scattering angle θ, for the 0°-geometry experiments. Neutron energy spread is indicated by the shaded area. On the right-hand side of the figure the energy spread increases discontinuously for the 7-foot-diameter Fe sample.

[20] E. R. Graves and R. W. Davis, Phys. Rev. **97**, 1205 (1955).
[21] A Monte Carlo theory for these calculations was developed by Herman Kahn and the calculations were carried out under his supervision at the Rand Corporation laboratories, Santa Monica, California.
[22] F. Bjorklund and S. Fernbach, Phys. Rev. **109**, 1295 (1958); also private communication.
[23] Graves, Rodrigues, Goldblatt, and Meyer, Rev. Sci. Instr. **20**, 579 (1949).
[24] S. J. Bame, Jr., and J. E. Perry, Jr., Phys. Rev. **107**, 1616 (1957).
[25] Calculations of multiple scattering of deuterons within the thick target were carried out by R. G. Thomas at this laboratory.

averaging and interpolating of such data the values of f_1 and f_2 were determined, $f_1(\phi,\alpha)$ being a correction for the yield in the direction of the detector during the count C, and $f_2(\theta/2)$ being a correction for the average yield over the surface of the scattering sample. The correction factor f_1/f_2 never differed from unity by more than 4%.

IV. SCATTERING SAMPLES AND SHADOW BARS

The cylindrical shells used as scattering samples ranged in diameter from 1 to 34 inches and in length from 2 to 8 inches, except for the largest ring of Fe which was 83 inches in diameter and 36 inches long. Radial wall thickness was chosen to keep the correction factor $\exp(p/\lambda_X)$ in the neighborhood of 1.05 to 1.10. Thicker samples were considered undesirable because of the increased multiple scattering.

In general the rings were sufficiently rigid to maintain their circular shape with the aid of several radial spokes of piano wire. However, the larger Pb and Sn samples were supported with additional thin steel rims, duplicates of which were set in place when the scattering ring was removed for a background run.

Chemical analysis[26] was made for suspected impurities in the scattering samples. In a few measurements impurities may have contributed a maximum of 3% error in $\sigma_e(\theta)$. For example, at the first minimum for Pb (see Fig. 6) a possible 0.2% Sb impurity would constitute a 2 to 3% contribution to $\sigma_e(\theta)$. No corrections for impurities were made.

The tungsten shadow bars were 1, $\frac{1}{2}$, or $\frac{3}{8}$ inch in diameter and 7 to 28 inches long. Choice of dimensions for a particular condition was made to minimize the background count. Although transmission through a 14-inch long bar was not significant, it was found appreciably better to use a longer bar when the geometry permitted. In general, the ends of the shadow bar extended as near as possible to the source and detector without shadowing any of the scattering ring. No doubt some neutrons were scattered toward the scattering ring by the end of the shadow bar near the neutron source. An attempt to observe the magnitude of this effect was made for several typical geometries by placing the detector at the position of the scattering ring and comparing the count with the shadow bar in place and then removed. The increase in count was not observable and was less than 1% over the whole spectrum of pulse heights observed.

V. NEUTRON DETECTORS

Neutrons were detected in small organic scintillators in which recoiling protons gave rise to light pulses viewed by a photomultiplier. Most of the measurements for scattering angle $\theta>40°$ were made with liquid scintillators, $\frac{1}{4}$, $\frac{1}{2}$, or $\frac{3}{4}$ inch in diameter, the larger detectors being used with large-diameter scattering rings where over-all angular resolution was not spoiled by a relatively large detector. For $\theta<40°$ most of the measurements were taken with cylindrical *trans*-stilbene crystal detectors, $\frac{1}{4}$ inch in diameter. Stilbene was not useful at large angles because its pulse-height response is markedly dependent on the direction of incidence of the neutrons. This characteristic prevented the response of the detector from having azimuthal symmetry which is essential in the cylindrical geometry employed in the experiments.

VI. COUNTING PROCEDURES AND DATA REDUCTION

In all measurements, the upper third of the pulse-height spectrum from the recoil-proton detector was recorded in an 18-channel analyzer. Figure 3 shows a typical set of spectra for the counts A, B, C, and the "net" count $A-B$. To deduce cross sections from the 0°-geometry data, values of the ratio $R=(A-B)/C$ were determined for the counts observed in each channel, and these ratios were then plotted *vs* pulse height as shown for a typical example in the lower part of Fig. 4. In general, R would fall with increase in pulse height to a plateau level which was interpreted as being characteristic of pure elastic scattering, the higher values at lower pulse height being due to the onset of inelastic scattering. The plateau value, shown by the dashed line in Fig. 4, was used to evaluate elastic scattering cross sections. This procedure, used to dis-

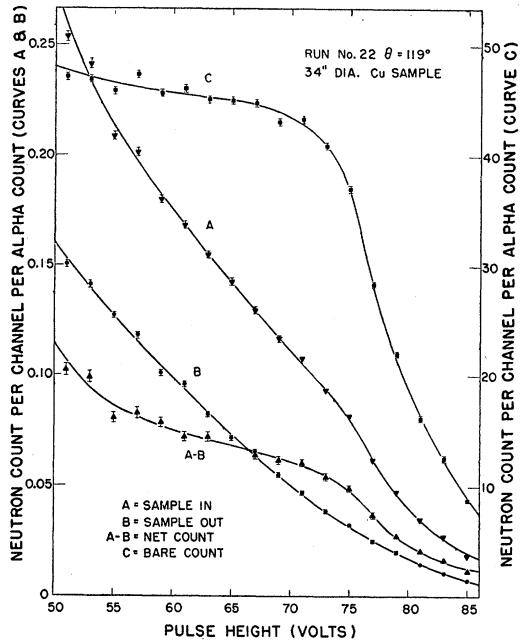

FIG. 3. Pulse-height spectra for the various conditions for which counts were observed in the recoil-proton neutron detector. Measurement of the direct neutron beam is curve C. This figure shows a typical set of data for which 6×10^6 alpha counts were registered to obtain each one of curves A and B.

[26] Careful chemical analyses were carried out by W. H. Ashley of the Chemistry Division at Los Alamos.

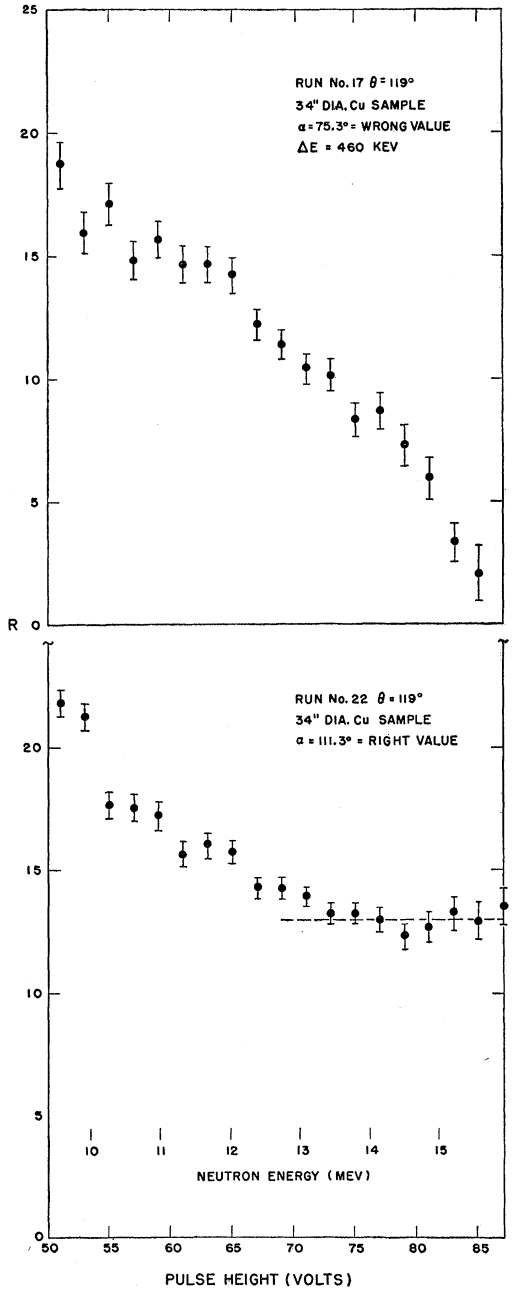

FIG. 4. The ratio $R=(A-B)/C$ *vs* pulse height for a typical set of data (lower) and for the same conditions altered to simulate an inelastic neutron group from a 460-kev level (upper). See text for meaning of "wrong value" of α. The energy scale runs up to fictitiously high values because of energy spread in the neutron source and broad instrumental energy resolution.

criminate against inelastically scattered neutrons, was not employed in the early 90°-geometry measurements where R was determined simply by using the total counts above a particular threshold. However, the simpler procedure was adequate in the region of angles less than 70°, where it was employed, and gave values in agreement with those obtained by the more elaborate procedure.

Several significant features of the raw data can be visualized on Fig. 3 and the lower part of Fig. 4 which displays the same set of original data. The signal-to-background ratio $(A-B)/B$ for this example is seen to be a little more than unity in the region of the plateau ($\sim$80 volts) on the plot of R *vs* pulse height. In other measurements $(A-B)/B$ varied from 10 in the best data to about 0.2 in the worst cases. The ratio B/C of the counts with and without the shadow bar for the present example is about 0.001 in the pulse-height region near the middle of the plateau. Values of B/C in this region ranged from a maximum of 0.006 downward by a factor 10. For this reason backgrounds were considered negligible compared with the direct beam count C.

As mentioned previously, in measurements with 0° geometry, when the count C was observed, the detector was rotated around the T(d,n) source to an angle α such that the neutron energy was equal to the energy of the elastically scattered neutrons. With each α setting, the detector was also turned through a polar angle β on a vertical axis through the center of the detector. The magnitude of β was $\theta/2$ and therefore the angle of incidence on the detector of primary neutrons from the source was the same as the angle of incidence of neutrons when scattered from the ring samples during the count A. With this procedure a correction for a small dependence of sensitivity on the angle β was unnecessary.

In order to account for the degradation in energy of the neutrons during elastic scattering in the 90°-geometry experiments, the count C was corrected by using a detector efficiency *vs* energy function $\epsilon(E)$, measured in auxiliary experiments by moving the detector to different angular positions around the T(d,n) source. The maximum correction made by this method was 30% (for C at 60°) where the uncertainty in the correction was estimated to introduce an error of 10% in the differential cross section. Most of the corrections were much less. In fact, for Cu, Sn, Pb, and U the corrections were less than 5% at all angles.

It should be noted the plateau value of R is determined from counts observed near the upper end of the pulse-height spectrum, where the direct beam count C is rapidly falling. It might be expected that the shape of the pulse-height spectrum in this region would be sensitive to the existing differences in the neutron energy spectra for those neutrons used at different angles α around the T(d,n) source. For example the energy spread of neutrons emitted near 90° is much less than the energy spread near 0° or 180°. The magnitude of this effect was studied by comparisons of the shape of the pulse-height spectra under radically different conditions, and it was estimated that the error introduced by this effect in the determination of the true plateau value of R was at most 5% in a few isolated cases.

VII. EXPERIMENTAL SEPARATION OF ELASTIC AND INELASTIC SCATTERING OF NEUTRONS

Differential cross sections $\sigma_{n,n^1}(\theta)$ for inelastic scattering were evaluated by replacing the plateau value of R in Eq. (1) by the difference between the value of R at 50 volts pulse height (see Fig. 4) and the plateau value; an approximate detector sensitivity correction was also made. This procedure lumps together the high-energy end of the inelastic scattering spectrum. Over this spectrum neutrons were detected with variable sensitivity as shown in Fig. 5 by the solid curve which is the calculated sensitivity for detection in the 50-to-52-volt channel. This sensitivity curve is normalized to unity for the elastically scattered neutrons. If one approximates the sensitivity curve by a rectangle as indicated in Fig. 5, the threshold of sensitivity is about 9.0 Mev, and the average sensitivity in the region 9 to 14 Mev is 1.4, which is the sensitivity correction factor referred to above. In applying this sensitivity correction, the simplifying assumption is made that the spectrum of inelastic neutrons is flat between 9 and 14 Mev. This assumption is certainly not strictly true because the energy levels involved are neither uniformly nor closely spaced. However, the error introduced in the inelastic scattering cross section is probably not more than 20%.

The question arises whether the elastic scattering cross section values include some of the highest energy inelastically scattered neutrons. In order to measure the over-all capability of the experiments to discriminate against inelastically scattered neutrons, a set of data was taken in which the count C was observed with the detector set at the "wrong" angle α so that the neutron energy was too high by 0.46 Mev. The plot of R for those data is given in Fig. 4, along with another set of data previously referred to, where conditions were identical except the detector was set at the correct angle. The data taken at the wrong angle simulate a hypothetical situation in which there is a single inelastically scattered group of neutrons from a 0.46-Mev energy level, and no elastically scattered group. It is seen that in this case there is no plateau value of R. From analysis of data of this kind it was estimated that a 20% admixture of inelastic scattering with 0.5-Mev energy loss would be observed and to a large extent separated from the elastically scattered group, whereas a 10% admixture would sometimes not be observed because of statistical error, electronic gain fluctuations, etc.

There is further evidence against there being as much as a 10% admixture of inelastically scattered neutrons included with the elastically scattered group except in case of U. For all the elements measured except U, the lowest known levels are in excess of 0.6 Mev except for a few rare isotopes. The calculated energy dependence of the sensitivity of the detector in the one analyzer channel from 78 to 80 volts (the middle of the plateau in Fig. 4) is shown as the dotted curve in Fig. 5. It is obvious from this curve that existing inelastic scattering

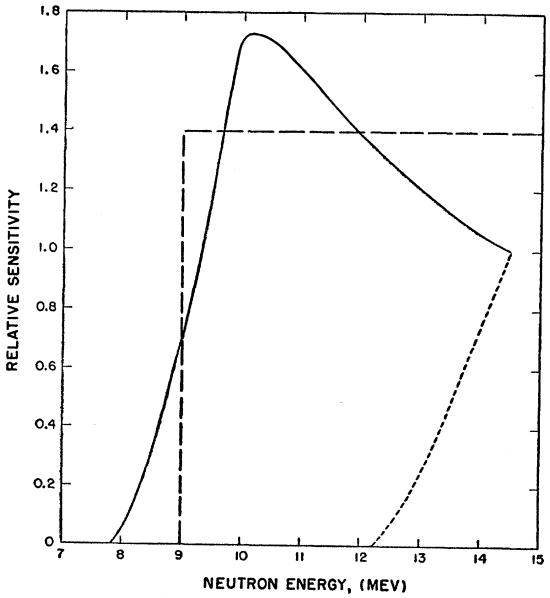

FIG. 5. The solid curve is the calculated detection sensitivity *vs* neutron energy for detection in the 50-to-52-volt channel of the pulse-height analyzer. Inelastically scattered neutrons of different energies were detected with this relative sensitivity variation. The dotted curve is the calculated detection sensitivity in the 78-to-80-volt channel. Both curves are normalized to unity at the energy of the elastically scattered neutrons.

contributions from the 0.045- and 0.14-Mev levels in U are included with essentially 100% efficiency in our elastic scattering cross sections. On the other hand, it is also seen from this curve that contributions from levels above 2 Mev are completely discriminated against. Anticipating the quantitative results given in Sec. XII, we find that the measured inelastic scattering cross sections for all neutrons of energy greater than 9 Mev are everywhere less than or equal to the elastic scattering cross section. In the case of Sn, for example, they are equal at the minima occuring at 80° and 120° in the elastic scattering cross-section curves. The neutron energy region above 9 Mev corresponds to inelastic scattering from levels up to 5.5 Mev. Therefore if all the energy levels contributed equally, the fact that the energy level density increases rapidly with excitation energy would mean that the levels below 2 Mev would indeed have negligible effect on the elastic scattering cross sections. If, on the other hand, the neutron energy spectrum tends to be flat by virtue of relatively strong contribution of the low-lying levels, then levels near 1 Mev would contribute about 10% to the elastic scattering cross section for the worst cases mentioned above for tin. Of such a 10% contribution only part would be separated from the elastically scattered group by the choice of the plateau level in plots of the type shown in Fig. 4.

If one assumes the trends for inelastic scattering with small energy loss are similar for neutrons at 14 Mev and protons at 18 Mev, the proton scattering data of Dayton

and Schrank[4] can be used as a basis for estimating the intensity of inelastic neutron scattering from single low-lying levels. These estimates turn out to be of the same order of magnitude as those indicated above.

To summarize, we estimate that except for U the inelastic scattering contribution to our elastic scattering cross section values is usually less than 5%, though in a few cases it may be as much as 10%, the largest contributions being at the minima of large-angle scattering. Uranium is an exception because of its low-lying levels, contributions from which, whether significant or not, are included in our elastic scattering cross-section values.

VIII. DISCRIMINATION AGAINST GAMMA RADIATION

The increase in the ratio $R=(A-B)/C$ with decrease in pulse height is due principally to the presence of inelastically scattered neutrons. But in some instances this increase may be due in part to gamma rays produced by neutron interactions in the scattering sample. The lowest energy of the recoiling protons whose pulses are recorded in the 18-channel analyzer with its threshold set at 50 volts is about 9 Mev. Because of the detector's relatively high scintillation response to electrons, the electrons produced by gamma rays of energies above 5 or 6 Mev would be detected if their full energy was expended within the scintillator. The range of 6-Mev electrons in the liquid scintillator is comparable to the dimensions of the $\frac{3}{4}$-inch detector and certainly exceeds that of the $\frac{1}{2}$-inch and smaller detectors. Therefore only gamma rays of energy about 6 Mev or greater would yield pulses large enough to be recorded.

Gamma radiations produced by the interactions of of 14-Mev neutrons with many elements have been investigated by Scherrer *et al.*[27] and Battat.[28] In order to make comparisons with these data, an experimental study of the absolute sensitivity of the detectors to the well-known 6-Mev gammas from $F^{19}(p,\alpha)O^{16}$ and 12-Mev gammas from $B^{11}(p,\gamma)C^{12}$ was carried out. The results of this study indicate that the background arising from gamma rays could not exceed one percent for the neutron elastic scattering cross-section data.

As an additional check of the possible effect of gamma-rays produced in the scattering rings, the values of the ratio R obtained with the $\frac{1}{2}$-inch and the $\frac{3}{4}$-inch detectors were compared in an attempt to discover systematic differences. Because the ratio of the detection efficiency for gamma rays to that for neutrons is larger in the $\frac{3}{4}$-inch detector, a significant background of gamma radiation would tend to increase the values of R in the region of small pulses more strongly when the large detector was used. In a number of cases, data had been taken for the same element and scattering angle with both detectors. Fifteen such cases were examined and no significant difference in the results obtained with the two detectors was observed.

Although these gamma-ray studies indicate negligible effects for the elastic scattering measurements, it was estimated that the experimental inelastic-scattering cross sections may have a small gamma-ray contribution not exceeding 10%.

IX. MULTIPLE-SCATTERING CORRECTION

Monte Carlo calculations of multiple scattering were made[21] for some of the Cu and Pb data for scattering angles between 5° and 70°. Scattering events were followed until the neutron escaped from the scattering ring, or had suffered an inelastic collision, or had suffered up to 5 elastic collisions. The number of neutrons suffering more than 5 elastic collisions was assumed negligible. The ratio of the calculated number of neutrons detected after 2 to 5 elastic collisions to the number detected after only one collision varied from 0.03 to 0.6. Ratios greater than 0.2 were rare, occurring only at angles near the deep first minimum in the $\sigma_e(\theta)$ curve for a given element. In general the Monte Carlo calculation was continued until the statistical error in the above-mentioned ratio was about 10%.

Corrections for multiple scattering for all elements have been applied by graphical interpolations and extrapolations of the calculations for Cu and Pb. However these corrections have been made only out to about 80° scattering angle where the corrections become only a few percent. Typical errors of 2% in $\sigma_e(\theta)$ may be attributed to uncertainty of the multiple-scattering corrections, though occasionally the error may be as large as 10%, especially at the deep first minimum.

X. ANGULAR RESOLUTION AND EFFECTIVE ANGLE

The experimental angular resolution varied from $\pm 1°$ to $\pm 3°$ total width. This is the sum of contributions due to finite size of source, detector, and scattering ring. Distortion of the $\sigma_e(\theta)$ curves due to this angular spread is probably significant only at the sharp first minima for Pb and U, where the $\sigma_e(\theta)$ values may be too high by a factor 1.5 or more.

If θ is the scattering angle for neutrons traversing the path between center of source, central element of scattering ring, and center of detector, then the average scattering angle $\bar{\theta}$ is slightly larger than θ because the angle is greater for a neutron scattered from either end of the ring. In fact, numerical calculations show that to a close approximation, $\bar{\theta}=\theta+\frac{1}{3}\Delta\theta_s$, where $\Delta\theta_s$ is the difference in scattering angle at the center and ends of the ring. With this correction the angles are estimated to be accurate to within a few tenths of a degree.

XI. ERRORS IN $\sigma_e(\theta)$ AND $\sigma_{n,n^1}(\theta)$

Errors in $\sigma_e(\theta)$ are due chiefly to three sources: statistical counting errors, errors in the multiple-

[27] Scherrer, Theus, and Faust, Phys. Rev. **91**, 1476 (1953); **89**, 1268 (1953).

[28] M. E. Battat, Los Alamos Report LA-1507, 1953 (unpublished).

scattering correction, and detection of inelastically scattered neutrons. These errors are smallest in the angular region covered by most of the first and second maxima, where average estimated errors are 5%. Errors are larger in the 5° intervals near the first and second minima and in the region of large-angle scattering ($\theta \geqq 90°$) where the average estimated error is 10%. At the first sharp minimum for Pb and U the errors are greatest and are estimated to be 50% when the effect of angular resolution is included. Angular resolution probably contributes negligible error elsewhere. At the larger angles measured for the lighter elements, namely C and Al, there were significant errors in the correction applied for the sensitivity of the detector *versus* neutron energy.

Errors in the integrals of the $\sigma_e(\theta)$ curves depend almost entirely on the more accurate data where cross-section values are large and where the errors are estimated to be 5%. Therefore the errors in the integrated elastic scattering cross sections are also estimated to be 5%.

There are three principle sources of error in the inelastic scattering cross sections: statistical counting error, uncertainty in the energy spectrum of the inelastic neutrons with the resulting uncertainty in the relative detector sensitivity discussed in Sec. VII, and error introduced by variation of the threshold for detection of the inelastically scattered neutrons. A few remarks should be made regarding the last mentioned of these sources of error. Small changes in electronic gain were accompanied by a shift in detection threshold. These shifts were significant in spite of gain readjustments, which were made by locating the rapidly falling portion of the pulse-height spectrum in the same channels of the analyzer. The combined error for the inelastic scattering cross sections is estimated to be 40% in the ordinate of the smoothed differential cross-section curves.

XII. RESULTS

The experimental differential elastic scattering cross sections are the data points shown in Fig. 6. As is noted in the caption of the figure, the energy scale at the top applies to some of the data points but not to others. Also shown in Fig. 6 are recent preliminary Livermore data[17] for C in the angular range from 40° to 150°, overlapping the present data in the region 40° to 55°. Livermore data for Pb, Sn, and Cu at angles greater than 140° are also shown to indicate the shape of the experimental curves at angles larger than were covered in our measurements.

As an indication of internal consistency and of the sensitivity of our data to neutron energy variation, Fig. 7 presents Pb data for 14.1- and 14.8-Mev neutrons in the region of small angles. The solid and dashed curves are the theoretical curves of Bjorklund and Fernbach[22] calculated for two energies, 14.0 and 15.0 Mev. Close inspection shows the experimental data

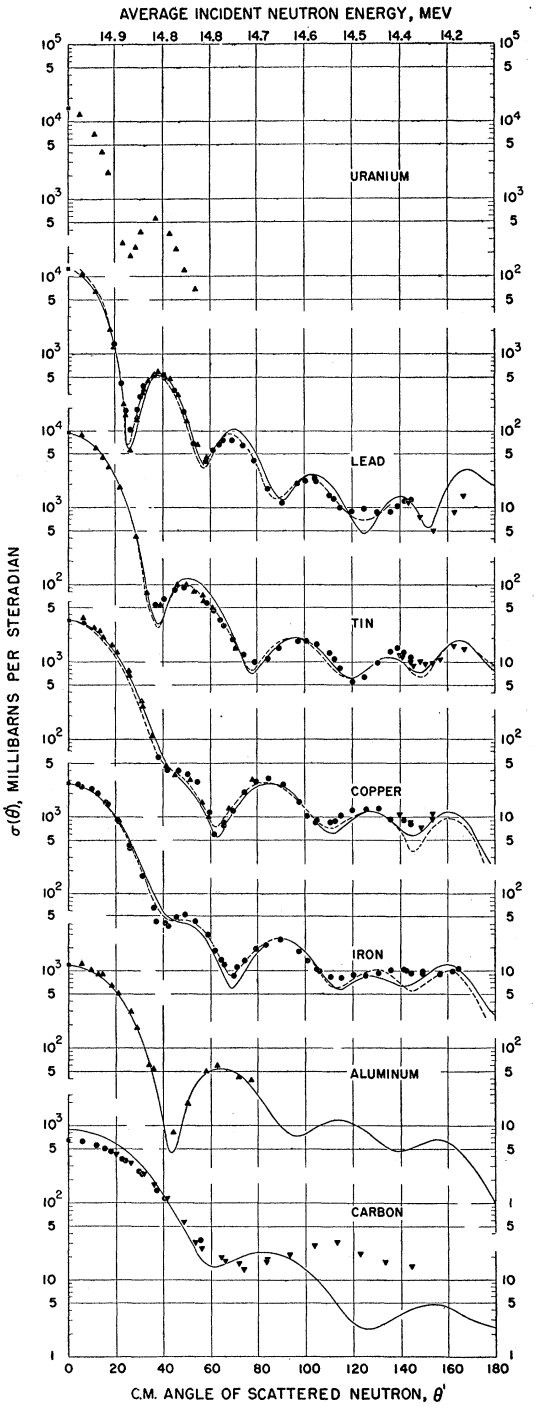

FIG. 6. Differential cross sections for elastic scattering of ~14.5-Mev neutrons. For the 0°-geometry data, shown by solid circles, the average primary neutron energy varies over a small range as indicated on the scale at the top of the figure. For the 90°-geometry data, shown by upright triangles, the average primary neutron energy is 14.1 Mev. The inverted triangles are Livermore data,[17] their *C* data being taken at 14.2 Mev and the other data at 14.6 Mev. The solid and dashed lines are theoretical curves of Bjorklund and Fernbach[22] derived for 14.0- and 15.0-Mev neutrons. Points at 0° are Wick's limit.

definitely shift slightly to the left at the higher energy, in qualitative agreement with the shift of the theoretical curves.

Where direct comparison can be made for the same element and angular range, the present results are in good agreement with data obtained at Livermore[17] and at NRL.[3,13] This agreement is significant in view of the fact that the Livermore and NRL experiments included neutrons of energy greater than 12 Mev whereas we have included only neutrons of energy greater than 13.5 or 14 Mev.

There is also good agreement between our data for Pb and NRL data for Bi. The cross sections for Bi and Pb apparently differ by an amount less than the experimental errors. This is not surprising because they are neighboring elements with very closely the same total[29] and nonelastic[20] cross sections. The Chalk River data[3,12] for Bi also agree well with the present data for Pb in the angular range out to about 80°, but for larger angles the Chalk River data are higher sometimes by a factor 2 or 3. Similarly, in the region beyond 80° the Chalk River data for Cd are about a factor 2 higher than the Livermore data for Cd. Part of these discrepancies may be due to the detection of inelastically scattered neutrons in the Chalk River measurements at large angles. This is to be expected if the detector threshold was 11 Mev as reported.[12] The Chalk River data for Ca and Mg probably do not have a significant inelastic scattering contribution because there are no low-lying energy levels in the abundant isotopes of these elements. For example the 97% Ca^{40} isotope has its lowest level at 3.35 Mev.

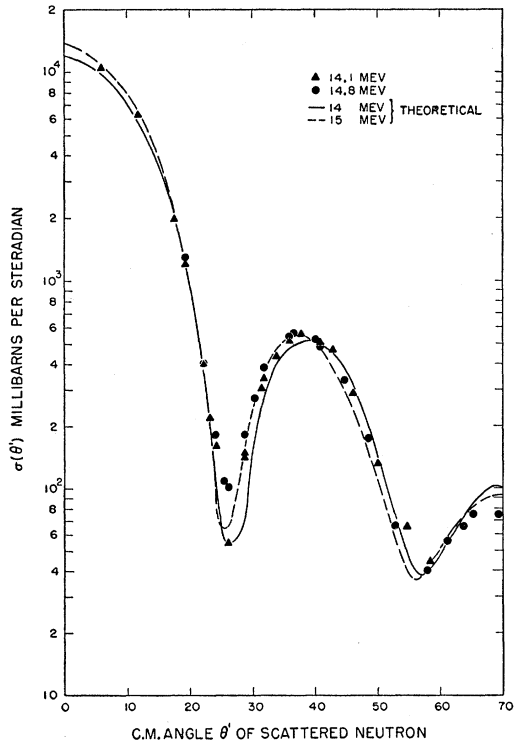

Fig. 7. Differential cross sections for elastic scattering of 14.1- and 14.8-Mev neutrons by Pb compared with theoretical curves of Bjorklund and Fernbach at 14.0 and 15.0 Mev.

[29] Coon, Graves, and Barschall, Phys. Rev. **88**, 562 (1952); J. P. Conner, Phys. Rev. **109**, 1268 (1958).

A close comparison of the various data for the sequence of neighboring elements Ag, Cd, In, and Sn shows remarkable similarity, with evidence of the expected progressive transitions in the differential cross-section curves.

Nauta[14] has made measurements for Pb, Hg, and Zn from 15° up to angles in the neighborhood of 90°, though his errors are as large as a factor 2 at the larger angles. His data for Pb are in reasonably good agreement with the present data. Mehlhorn's[3,15] preliminary data on large-angle scattering (90° to 150°) of 13.7-Mev neutrons by Pb lie everywhere lower than the present data by a factor 2 to 3, except at 90° where there is agreement.

Smooth curves drawn through the experimental points of Fig. 6 and extrapolated smoothly to 0° and 180°, were integrated to obtain the elastic-scattering cross sections σ_e tabulated in Table I. The incomplete curves for U and Al were terminated at 50° and 80° and the partial elastic scattering cross sections σ_e (partial) were evaluated up to these angles. Also tabulated in Table I are the known total cross sections[29] σ_t, nonelastic cross sections[20] σ_X, and the difference $\sigma_t-\sigma_X$ which is seen to be in good agreement with σ_e for Pb, Sn, Cu, Fe, and C. For U and Al the value of $\sigma_t-\sigma_X-\sigma_e$ (partial) may be considered as a rough experimental value for elastic scattering through angles greater than 50° for U, and greater than 80° for Al.

Wick[30] has set a theoretical lower limit to the differential elastic-scattering cross section at 0°, the limit being given by $\sigma_e(0°)\geqq(k\sigma_t/4\pi)^2$. This quantity represents the contribution of only the imaginary part of the scattering amplitude. It is therefore somewhat surprising that this lower limit (see Fig. 6) is on a smooth extrapolation of the $\sigma_e(\theta')$ data, within experimental error. However, an optical-model calculation at this laboratory by Porter[31] was made for 13 values of A between 8 and 240 to compare the magnitude of the real and imaginary contributions to $\sigma_e(0°)$. A Saxon-type potential was employed with real and imaginary potentials of 44 and 5.3 Mev, a nuclear radius of $1.33A^{\frac{1}{3}}\times10^{-13}$ cm, and an exponential fall-off distance of 0.5×10^{-13} cm. The contribution of the real part was found to be at most a few precent of the imaginary contribution. This result means that at 14 Mev the Wick limit value is not only a lower limit but is very

[30] G. C. Wick, Atti reale accad. Italia, Mem. classe sci. fis., mat. e nat. **13**, 1203 (1943).

[31] This calculation was carried out in the Theoretical Division at Los Alamos using an IBM-704 computer. An existing code prepared by William Anderson was modified slightly to allow separate observation of the real and imaginary contributions.

TABLE I. Integrated elastic and inelastic scattering cross sections. Comparisons are shown of the integrated elastic scattering cross sections and the differences between known total cross sections σ_t and nonelastic cross sections σ_X. Values of σ_t and σ_X are taken from references 32 and 20, respectively. In reference 20 a quantity σ_i is defined as the cross section for all nonelastic processes plus, for light elements, a small amount of large-angle elastic scattering; for carbon, $\sigma_i=0.60$ barn of which 0.05 is estimated to be elastic scattering; therefore $\sigma_X=0.55$ barn.

Element	Angle range for elastic scattering	$\int\sigma_e(\theta)d\Omega$ (barns)	σ_t (barns)	σ_X (barns)	$\sigma_t-\sigma_X$ (barns)	$\int_{9\text{ Mev}}^{14\text{ Mev}}\int_{40^\circ}^{180^\circ}\sigma_{n,n1}(\theta)d\Omega dE$ (millibarns)
C	0–180	0.77±0.04	1.31±0.02	0.55±0.02	0.76±0.03	
Al	0–80	0.67±0.03	1.73±0.03	1.00±0.01	0.73±0.04	
Fe	0–180	1.14±0.06	2.50±0.05	1.27±0.04	1.23±0.07	76±30
Cu	0–180	1.45±0.07	2.96±0.06	1.42±0.04	1.54±0.07	72±30
Sn	0–180	2.59±0.13	4.68±0.09	1.96±0.05	2.72±0.10	91±30
Pb	0–180	2.83±0.14	5.40±0.08	2.49±0.02	2.91±0.09	88±30
U	0–50	2.73±0.14	5.87±0.12	2.73±0.04	3.14±0.13	

nearly equal to $\sigma_e(0°)$. In Fig. 8 it is seen that the Wick limit values computed from experimental σ_t values are, within the rather large experimental errors, equal to the "experimental" values of $\sigma_e(0°)$ obtained by arbitrary smooth extrapolation of the $\sigma_e(\theta)$ data to 0°. At the present stage of experiment and theory, of one ignores the so-called Schwinger scattering,[32] the best value of $\sigma_e(0°)$ at 14 Mev is probably Wick's limit. The Schwinger scattering which arises from the interaction of the neutron magnetic moment with the Coulomb field of the nucleus causes a sharp rise in the differential cross section at very small angles of less than 1°. This sharp rise has been verified experimentally[33] in the scattering of 4-Mev neutrons by Pb.

The curves shown in Fig. 6 are the calculations of Bjorklund and Fernbach[22] based on the optical model with the addition of a spin-orbit term of the Thomas type. The solid and dashed curves are their calculations at 14 and 15 Mev, respectively. Their potential has the form $V=V_{CR}\rho(r)+iV_{CI}q(r)+V_{SR}(\hbar/\mu c)^2r^{-1}(d\rho/dr)\boldsymbol{\sigma}\cdot\mathbf{l}$ where

$$\rho(r)=\{1+\exp[(r-R_0)/a]\}^{-1},$$
$$q(r)=\exp[-(r-R_0)^2/b^2],$$

and $R_0=r_0A^{\frac{1}{3}}$. For 14-Mev neutrons they find for the best over-all fit to experimental data $V_{CR}=44$ Mev, $V_{CI}=11$ Mev, $V_{SR}=8.3$ Mev, and in units of 10^{-13} cm, $a=0.65$, $b=0.98$, and $r_0=1.25$. The agreement between these theoretical curves and experimental data is seen to be fairly good except for C which is too small a nucleus for the theory to be applicable. In several cases (e.g., Fe and Sn in the forward hemisphere) the data agree much better with the theoretical curve for the more appropriate neutron energy. Their choice of the spin-orbit potential was based on shell-theory predictions. However, it would be highly desirable to carry out neutron polarization experiments[34] to serve as a basis for determining the spin-orbit term. In calculations made by Beyster[35] without the use of a spin-orbit term, the theoretical curves fit the data fairly well for angles less than 90°, but for larger angles the amplitude of the oscillations in the calculated curves is much too large, with discrepancies as large as a factor 10.

It is interesting to note that the above-quoted values of 44 and 11 Mev for the real and imaginary potentials are in approximate agreement with the potentials derived by Melkanoff *et al.*[36] from data on the elastic scattering of protons. To make this comparison it is assumed that the 14-Mev neutron is equivalent to a proton of energy ~22 Mev, which is approximately equal to the neutron energy plus the Coulomb barrier,

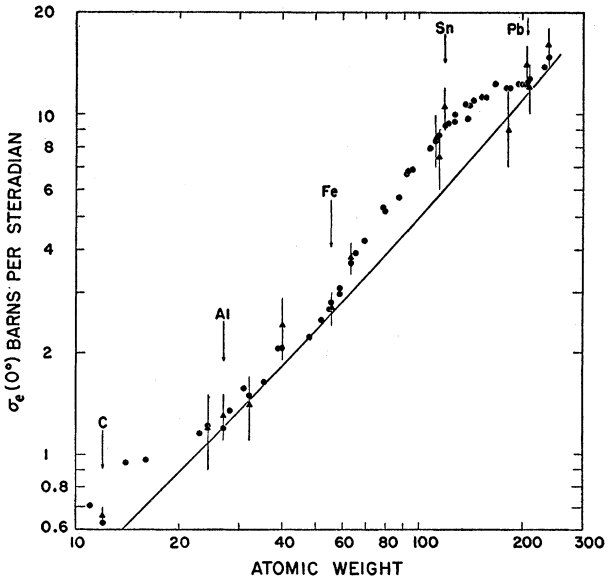

FIG. 8. Values of differential cross sections for elastic scattering of ~14.5-Mev neutrons at 0° *vs* atomic weight. ●=Wick's limit, $(k\sigma_t/4\pi)^2$ using experimental values of σ_t. ▲=extrapolation of available experimental $\sigma_e(\theta)$ data by arbitrary smooth curves. —=$(kR+1)^4/(4k^2)$ with $R=1.33A^{\frac{1}{3}}$.

[32] J. Schwinger, Phys. Rev. **73**, 407 (1948).

[33] Iu. A. Aleksandrov and I. I. Bondarenko, J. Exptl. Theoret. Phys. (U.S.S.R.) **31**, 726 (1956) [translation: Soviet Phys. JETP **4**, 612 (1957)].

[34] H. H. Barschall, *Proceedings of the International Conference on the Neutron Interactions with the Nucleus*, held at Columbia University, 1957 (to be published), Sec. IV-B1.

[35] J. R. Beyster, Los Alamos Report LA-2099, 1957 (unpublished).

[36] Melkanoff, Moszkowski, Nodvik, and Saxon, Phys. Rev. **101**, 507 (1956).

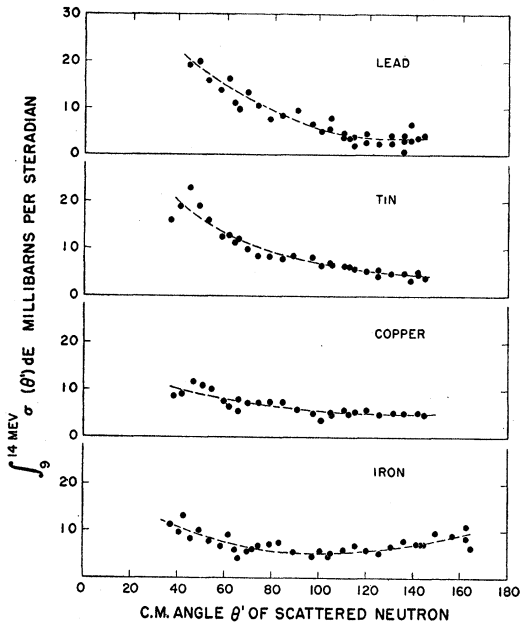

FIG. 9. Differential cross sections for inelastic scattering of ~14.5-Mev neutrons. Only neutrons emitted with energy greater than ~9 Mev were detected. The sensitivity with which neutrons of different energies were detected is the solid curve in Fig. 5.

though of course this quantity varies with nuclear charge. However, such a comparison is a gross oversimplification because, as was mentioned in Sec. I, neutrons and protons probably do not experience the same real potential in the nucleus. The value 11 Mev for the imaginary potential is also in agreement with the theoretical estimate of Lane and Wandel.[37]

Our experimental inelastic scattering cross sections are given in Fig. 9. In proceeding from heavy to lighter nuclei it is apparent that the curves become progressively flatter, and the curve for Fe has a minimum near 90°. Qualitative comparisons may be made between these experimental data and those of Rosen and Stewart,[38] and Ahn and Roberts,[39] who have made measurements on the yield of inelastically scattered neutrons from Bi, Ta, and Zr bombarded with 14-Mev neutrons. These experimenters lumped together the inelastically scattered neutrons of energies 4 to 12 Mev. Therefore their cross sections represent a wider energy band and lie everywhere higher than ours. Their data also show a progressive flattening toward lighter elements. Our higher-energy band of neutrons (9 to 14 Mev) is more strongly peaked forward than the lower-energy band (4 to 12 Mev), in agreement with the predictions of the direct-interaction hypothesis.[40]

Smooth curves drawn through the inelastic scattering cross section data points and extrapolated to 180° were integrated from 40° to 180°. This integration gave the values listed in Table I. Although a direct comparison is not possible, these values are somewhat higher than would be estimated from the data of Graves and Rosen.[41]

ACKNOWLEDGMENTS

We wish to thank A. E. C. Green and C. E. Porter for discussions of some of the theoretical implications, and Howard Bryant and J. M. Holt, Jr., for aid in developing some of the equipment and taking data.

[37] A. M. Lane and C. F. Wandel, Phys. Rev. **98**, 1524 (1955).

[38] L. Rosen and L. Stewart, Phys. Rev. **107**, 824 (1957).

[39] S. H. Ahn and J. H. Roberts, Phys. Rev. **108**, 110 (1957).

[40] R. M. Eisberg and G. Igo, Phys. Rev. **93**, 1039 (1954); S. T. Butler, Phys. Rev. **106**, 272 (1957); G. Brown and H. Muirhead, Phil. Mag. **2**, 473 (1957).

[41] E. R. Graves and L. Rosen, Phys. Rev. **89**, 343 (1953).